

Integrated D-InSAR and Ground-based Radar for Open Pit Slope Stability Monitoring and Implications for Rock Mass Young's Modulus Reduction

Faris Ridwan Maulana, Ridho Kresna Wattimena & Budi Sulistianto

Mining Engineering Department, Faculty of Mining and Petroleum Engineering, Institut Teknologi Bandung, Jalan Ganesha 10, Bandung 40132, Indonesia

Corresponding author: farisridma01@gmail.com

Abstract

Excavation and material stockpiling activities in the mining process cause a change in the distribution of forces and stresses in the material. As a result, the material will seek a new equilibrium by releasing the load through a landslide. As part of mitigation, it is necessary to monitor displacements occurring on slopes using high-accuracy devices. Ground-based radar is a technique considered to have good ability to detect displacements in real-time. However, ground-based radar has a weakness in that it cannot detect vertical displacement. One of the emerging technologies that is used for monitoring vertical displacements as LoS displacements is D-InSAR analysis. With the integration of both methods, displacements that occur horizontally and vertically on a slope can be detected properly. In addition, the decrease in rock mass strength due to displacement can be predicted based on numerical analysis using the finite element method. Monitoring was carried out from December 10th, 2021 to April 9th, 2022. The monitoring results from the beginning to the end of the period showed that the horizontal and vertical displacements that occurred in the low wall area were 1247.34 mm and 292.5 mm, respectively. Correlated with these conditions, the Young's modulus value of the rock mass decreased between 3% and 35%.

Keywords: *D-InSAR; ground-based radar; rainfall; rock mass; Young's modulus.*

Introduction

Mining activities, whether carried out using an open pit or underground mining, cannot be separated from the activities of excavating and dumping materials. The consequences of these activities can cause changes in the distribution of forces and stresses in the material. As a result, the material will seek a new equilibrium by releasing the load through rock mass avalanches. Instability in openings and slopes can cause various problems, from negative impact on the environment, damage to mining equipment, threatening the safety of workers, to mine closure due to economic aspects that are not on target [1]. As a part of a mitigation system, it is necessary to have good hazard risk management. One form of management is by integrating various methods to monitor areas that are considered critical. One of the parameters of concern is monitoring rock mass displacement. Various methods are used in monitoring displacement, ranging from conventional methods by direct survey of critical areas, to methods that use high-tech devices to monitor rock mass displacement.

The conventional method is carried out by surveying the critical area. A limitation of this method is that it is very dependent on weather conditions and can only be done during the day. Therefore, many companies have now switched to using more modern devices, one of which is Ground-based radar. This is one of the most effective and accurate tools for detecting rock mass displacement. Displacement information is provided in a few minute intervals with accuracy up to the millimeter scale with wide area coverage [2]. Although it has many advantages, it has one major weakness, which is that it cannot detect vertical displacement. Sensors ground-based radar can only detect the movement of rock masses that tend to approach or move away from the sensor.

Based on these conditions, it is necessary to integrate other devices or technologies that can detect vertical displacement with high accuracy. One of the developing technologies is utilizing the Sentinel-1 satellite to determine changes in the earth's surface condition through D-InSAR analysis by LoS displacement. Another

advantage of D-InSAR is that it can detect rock mass displacements less than 5 mm [3]. In addition, the waves emitted by the satellite to detect displacements do not require a reflector device, so the coverage area in the D-InSAR analysis is very wide. With the integration of both techniques, the displacement values that occur horizontally and vertically can be detected properly. Displacement in a rock mass is a form of decreasing the strength of the rock mass. By using the rock mass displacement value, a decrease in rock mass strength can be obtained based on numerical analysis with the finite element method. Information on displacements and the magnitude of the decrease in rock mass strength can be used as a reference in determining policies related to the safety and the operation of mining activities.

Literature Review

Types of Slope Movement

As a part of monitoring, it is important to know the mechanism of the rock mass displacement. This information will be useful to determine which equipment to use and the interpretation of the results of monitoring devices. Landslides that occur on slopes do not just happen at once. The occurrence of rock mass landslides is preceded by a slow rock mass movement, which is then followed by a landslide event. Therefore, it is important to know the characteristics of the rock mass movement occurring slowly. The relationship between rock mass displacement against time can be divided into three types [4].

The first type of slope movement is called regressive movement. The slope will tend to experience regressive movement, where the velocity of the rock mass displacement slows down until it reaches stability (Figure 1). The slope will become more stable as the ratio between the driving force and the resisting force decreases. The slope movement will continue to slow down until there are factors that can increase its velocity of movement. These factors can be in the form of blasting or changes in groundwater pressure due to high rainfall intensity. The progressive deformation trend is characterized by an increase in the velocity of the rock mass displacement. However, not all increases in velocity will lead to progressive deformation trend. The slope will only experience progressive if the discontinuity plane angle is steeper than the friction angle, which will cause the rock shear strength to decrease (Figure 1). As shown in Figure 1, with increasing time, the C curve, which initially experienced a regressive deformation trend, will turn into a progressive one. These changes in movement will cause a landslide. These changes can be triggered by an increase in groundwater pressure, rock excavation on the toe of the slope, or other factors that cause instability of the slope.

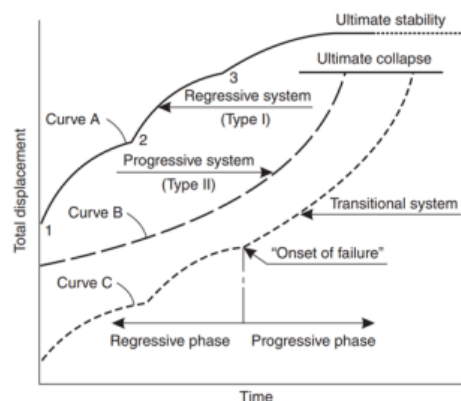


Figure 1 Rock mass displacement curve against time [4].

Differential Interferometry Synthetic Aperture Radar (D-InSAR)

Although radar technology has developed over fifty years, the components that support interferometric radar processing have been developed only about ten years ago. One of the uses of remote sensing technology, in the world of mining, especially D-InSAR, is as a means of monitoring slope stability. The principle used is to look for differences in the condition of the earth's surface at the same location in different acquisition data (Figure 2). In this case, the radar sensor will read the line of sight (LoS) component that appears when a displacement occurs.

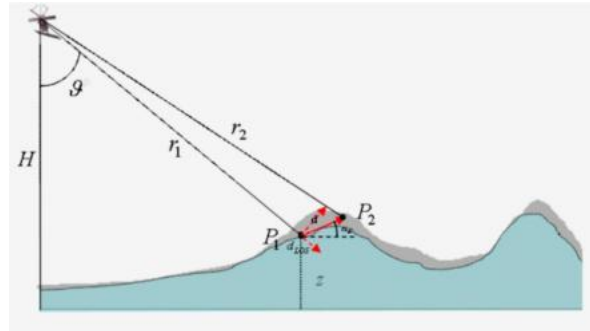


Figure 2 Illustration of D-InSAR analysis for surface displacements using line of sight (LoS) [5].

Information on displacements that occur on the earth's surface can be known based on imagery produced by satellite. In the images, there is information on the phase difference of the electromagnetic waves emitted and then received back by the satellite. Phase differences in electromagnetic waves occur due to changes in the conditions of the earth's surface, as shown in Figure 2. With targets that are only surface conditions, the coverage area of the monitoring method with D-InSAR is very wide. In addition, electromagnetic waves emitted by satellites can penetrate clouds and are not affected by weather conditions in the local area [6]. Although it has several advantages, the D-InSAR monitoring method, has one major disadvantage. Sentinel-1 data as raw data for D-InSAR analysis is available only at intervals of several days. Therefore, takes several days to obtain displacement information from the satellite-based data acquisition process. In addition, as a principle of monitoring with SAR interferometry, sensors on satellites can only find displacement information based on the trend of surface changes that are moving away from or approaching the sensor. Thus, the displacements obtained by D-InSAR analysis are only displacements that occur vertically.

Methodology

PT Adaro Indonesia is a coal mining company located in Tabalong Regency, South Kalimantan (Figure 3). The present study was conducted in the low wall area of pit South Tutupan, which is one of the areas included in the concession area of PT Adaro Indonesia. Two other locations that were also included in the PT Adaro Indonesia concession area were Paringin and Wara. The main product of PT Adaro Indonesia is Envirocoal, which is included in the sub-bituminous coal type with a calorific value in the range of 4000 to 5000 kcal/kg. In 2021, PT Adaro Indonesia's coal reserves amounted to 731 million tons with resources reaching 3.3 billion ton. In the same year, PT Adaro Indonesia's coal production reached 43.2 million tons with more than 70% coming from Tutupan.

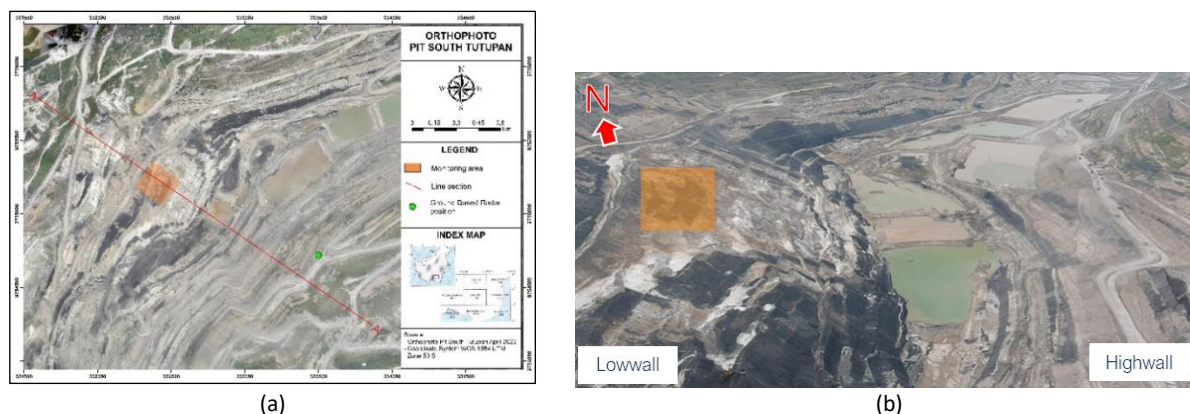


Figure 3 Area of South Tutupan min: (a) plane view; (b) camera directed to the north.

Because of high activities in the South Tutupan pit area, the company has determined various policies with high standards so that operations can run well and effectively. One of the policies made is related to the aspect of slope stability. Based on a survey the slope height on the low wall side of the South Tutupan pit exceeds 200 m. This makes the slope stability of the South Tutupan pit low wall area one of the main focuses of the company. Various methods and devices have been installed to monitor the stability of the low wall side slopes, one of

which is a rock mass displacement monitoring device. The displacement aspect is important because it is one of the indicators in determining policies related to mining operations. One of the displacement monitoring devices that has been used and has good accuracy is ground-based radar because it can provide information on the horizontal displacement of rock masses in real-time with measurement accuracy up to millimeters (mm). Data from ground-based radar monitoring is presented in Table 1 for the period from December 10th, 2021 to April 9th, 2022 with a monitoring interval of two hours. The graph in Figure 4 is a visualization of the horizontal displacement that occurred in the low wall pit area of South Tutupan.

Meanwhile, to identify LoS displacements in the low wall area, D-InSAR analysis was used based on Sentinel-1 data processing. The Sentinel-1 data used was open-source data with an interval of twelve days. The monitoring period was based on the availability of data between the ground-based radar data and the Sentinel-1 data. Therefore, monitoring was carried out from December 10th, 2021 to April 9th, 2022. In general, the concept of monitoring with D-InSAR is carried out by comparing two Sentinel-1 data from successive acquisition periods. If there is a change in the topographic conditions, there will be a phase difference in the electromagnetic wave which is interpreted as LoS displacement. To get the LoS displacement value, some processing must be done in the D-InSAR analysis using the Sentinel Application Platform (SNAP) software as illustrated in Figure 5 [7].

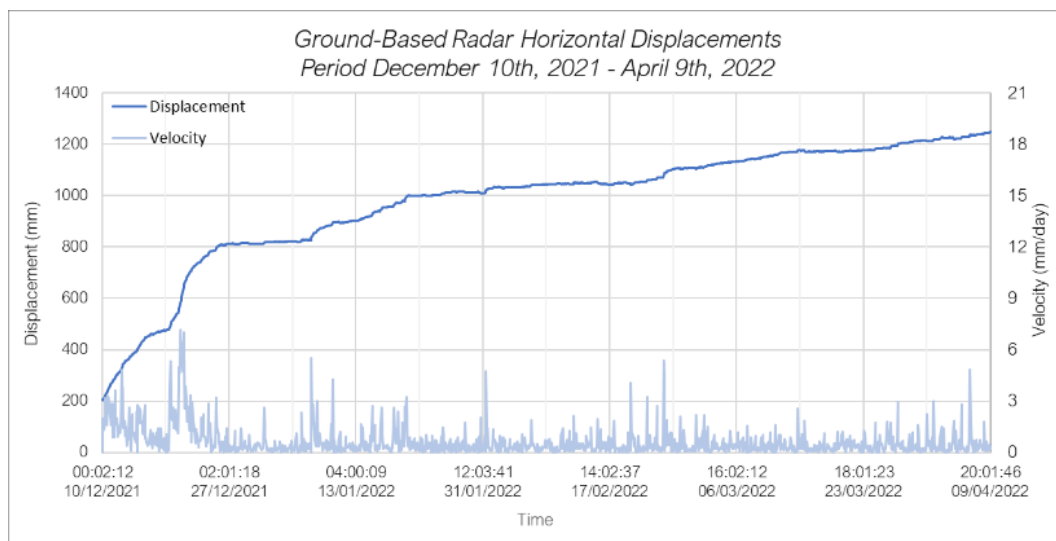


Figure 4 Correlation value and velocity of horizontal displacement in the low wall area.

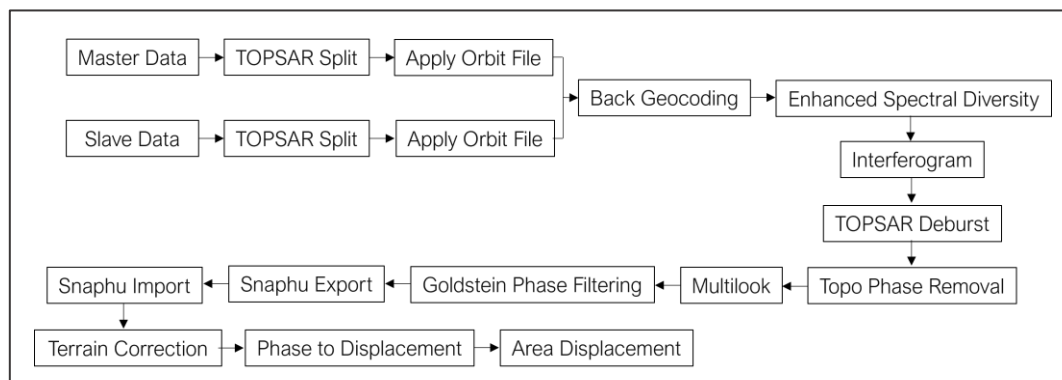


Figure 5 Sentinel-1 processing for D-InSAR analysis [7].

With the Sentinel-1 data used in the D-InSAR analysis, the LoS displacement value is obtained by processing the data as illustrated in Figure 5. One of the purposes of doing this processing is to remove noise arising from the Sentinel-1 data acquisition process. Noise that appears during data acquisition comes from interactions between electromagnetic waves and atmospheric conditions, which can produce ambiguity in the SAR data. This noise consists of two types, namely regional noise, and single-data anomalies. Regional noise is noise that appears on a wide scale and usually occurs in several data acquisition periods. One of the factors that cause this type of noise

is the difference in thermal conditions on the surface due to changes in weather and season. To detect the presence of this noise, a coherence value parameter is used. Pixels that show high deformation values and low coherence values (< 0.9) indicate that the detected deformation is affected by the presence of noise [7]. The type of noise that appears in one of the data (single-data anomaly) can be identified based on the approach taken to regional noise. If there are three or more data sets affected by high atmospheric conditions, the data can be replaced with data that has a low impact.

One of the rock mechanics parameters that affect rock mass displacement is Young's modulus. A decreasing Young's modulus value correlates with decreasing rock mass strength. To determine the decrease percentage, this study used finite element numerical modeling. The modelling was done by reducing the value of Young's modulus gradually until the displacement value obtained from the numerical analysis was close to the actual displacement value from the monitoring results. To carry out this modelling, data are needed such as slope geometry, subsurface lithology sections, mechanical parameters of rock mass, and load borne by the slope. The slope geometry was created based on updated topographical conditions in the South Tutupan pit area, which were then made into a two-dimensional (2D) cross-section. This cross-section was made transversely from the low wall to the high wall are with a length of more than 2500 m.

Based on these conditions, it was found that the slope height reached 250 m with an overall slope of 20° . Then the subsurface lithology arrangement was input into the previously made cross-section. The load experienced by the slope is divided into two types, namely the seismic load and the pore pressure coefficient (R_u coefficient). Meanwhile, the rock types found in the South Tutupan pit area, especially in the low wall area, are three types of rock sandstone, mudstone, and coal with mechanical parameters as presented in Table 1. When all the modeling parameters were known, the two-dimensional slope model presented in Figure 6 was obtained.

Table 1 Mechanical parameters of lithology in the South Tutupan pit area.

Mechanical Parameters	Sandstone	Mudstone	Coal
Unit weight (kN/m^3)	20.25 - 22.00	20.00 - 24.26	12.45 - 21.80
UCS (MPa)	0.80 - 11.28	0.90 - 19.24	1.25 - 12.01
Young's modulus (MPa)	376.81 - 21209.10	557.51 - 15422.94	464.81 - 5284.63
Poisson ratio	0.217 - 0.224	0.261 - 0.274	0.217 - 0.224
Tensile strength (MPa)	0.0005 - 0.0455	0.0014 - 0.0660	0.0006 - 0.0074
Cohesion (MPa)	0.18 - 0.83	0.17 - 0.65	0.17 - 0.65
Friction angle ($^\circ$)	11.62 - 32.56	9.68 - 27.78	15.73 - 30.10

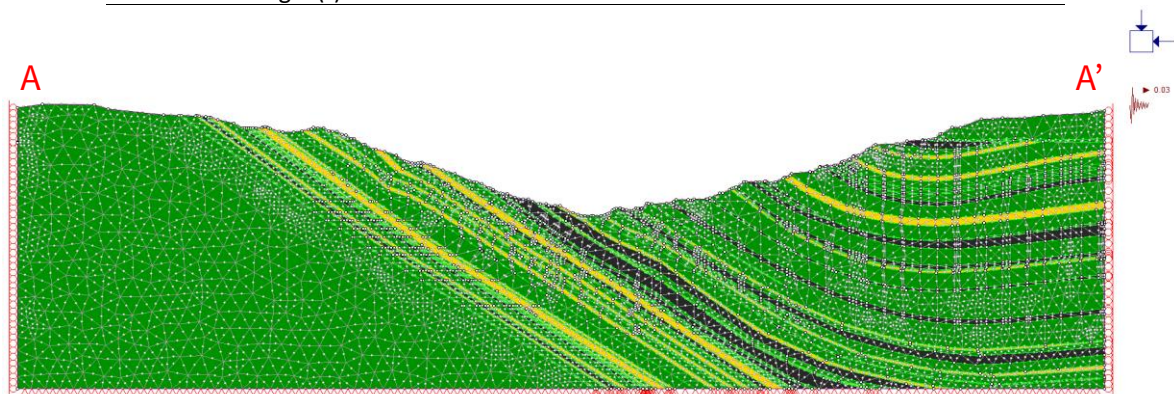


Figure 6 2D Cross-section A-A' in low wall area.

Results and Discussion

Horizontal Displacements Monitoring

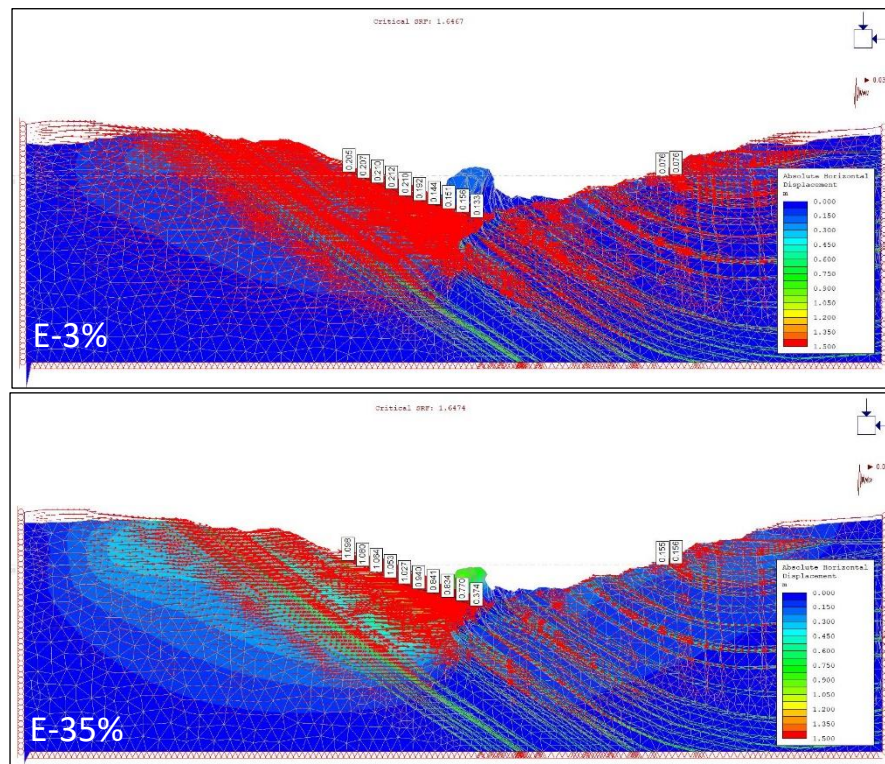
In this study, horizontal displacement monitoring was carried out using ground-based radar. Monitoring results in the form of displacement values were obtained in real-time. To get the same time interval as D-InSAR monitoring, a recap of the monitoring results was made with twelve-day intervals. The results of monitoring with ground-based radar are shown in Table 2.

Table 2 Horizontal displacement recap based on ground-based radar monitoring.

Date	Horizontal Displacement (mm)
12/10/2021	202.28
12/22/2021	737.59
01/03/2022	821.33
01/15/2022	938.53
01/27/2022	1013.79
02/08/2022	1044.68
02/20/2022	1050.47
03/04/2022	1128.49
03/16/2022	1171.74
03/28/2022	1204.60
04/09/2022	1247.34

Based on the monitoring results, there was an increase in the horizontal displacement from December 10th, 2021 to January 15th, 2022. On December 10th, 2021, the horizontal displacement value was 202.28 mm, while the horizontal displacement value on January 15th, 2022 was 938.53 mm. This shows an increase in the displacement value of 736.25 mm in an interval of 36 days. In the following period, the increase in the displacement value tended to be linear and did not experience a significant increase. The increase in the horizontal displacement value is shown in Figure 4. Furthermore, to determine the effect of the horizontal displacement on the rock mass characteristics, a numerical analysis was carried out using the finite element method. The analysis was carried out by varying the Young's modulus parameter for each type of material and applying the strength factor reduction (SRF) method. Varying the value of Young's modulus is considered good if the horizontal displacement from the numerical analysis is close to the horizontal displacement from ground-based radar monitoring.

Based on these assumptions, the horizontal displacement value from the numerical analysis on December 10th, 2021 was 281 mm, 205 mm in the low wall area and 76 mm in the high wall area with a reduction of the Young's modulus value of 3% compared to the initial value (Figure 7).

**Figure 7** Horizontal displacement based on numerical analysis by reduction of Young's modulus and applying the SRF method.

In the same period, the horizontal displacement value from the monitoring of the ground-based radar was known to be 202.28 mm. This method was used to determine the decrease of the Young's modulus value based on the displacement that occurred in the next monitoring period. The results obtained are presented in Table 3.

Table 3 Comparison of horizontal displacement based on ground-based radar monitoring and numerical analysis by reduction of the Young's modulus value and applying the SRF method.

Horizontal Displacement Monitoring (mm)		Horizontal Displacement Numerical Analysis (mm)			Critical SRF	Young's modulus Reduction
Date	GBR	LW	HW	Total		
12/10/2021	202.28	205.00	76.00	281.00	1.647	E-3%
12/22/2021	737.59	644.00	119.00	763.00	1.647	E-15%
01/03/2022	821.33	741.00	122.00	863.00	1.648	E-18%
01/15/2022	938.53	791.00	135.00	926.00	1.647	E-25%
01/27/2022	1013.79	888.00	139.00	1027.00	1.648	E-27%
02/08/2022	1044.68	894.00	140.00	1034.00	1.648	E-28%
02/20/2022	1050.47	904.00	142.00	1046.00	1.648	E-29%
03/04/2022	1128.49	984.00	144.00	1128.00	1.647	E-29.5%
03/16/2022	1171.74	1027.00	145.00	1172.00	1.648	E-30%
03/28/2022	1204.60	1033.00	151.00	1184.00	1.648	E-33%
04/09/2022	1247.34	1098.00	156.00	1254.00	1.647	E-35%

The regression results of the two horizontal displacement value produced an R-square value of 0.9992 (Figure 8). This shows that the horizontal displacement value of the results of numerical analysis and the results of monitoring were mutually correlated at 99.92%. In addition to the R-square value, from the regression results, other results were found by applying the following equation:

$$d_{hnum} = 1.0034d_{hGBR} \quad (1)$$

where, d_{hnum} is the horizontal displacement value as a result of numerical analysis, and d_{hGBR} is the horizontal displacement value based on ground-based radar monitoring.

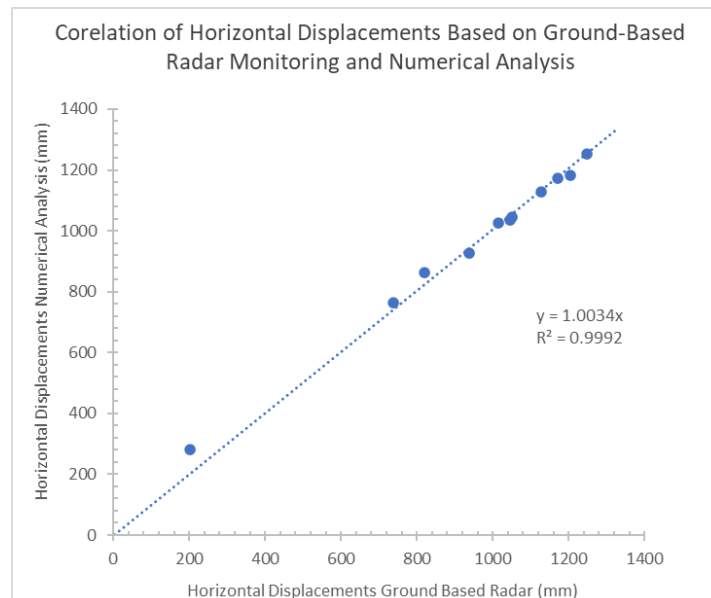
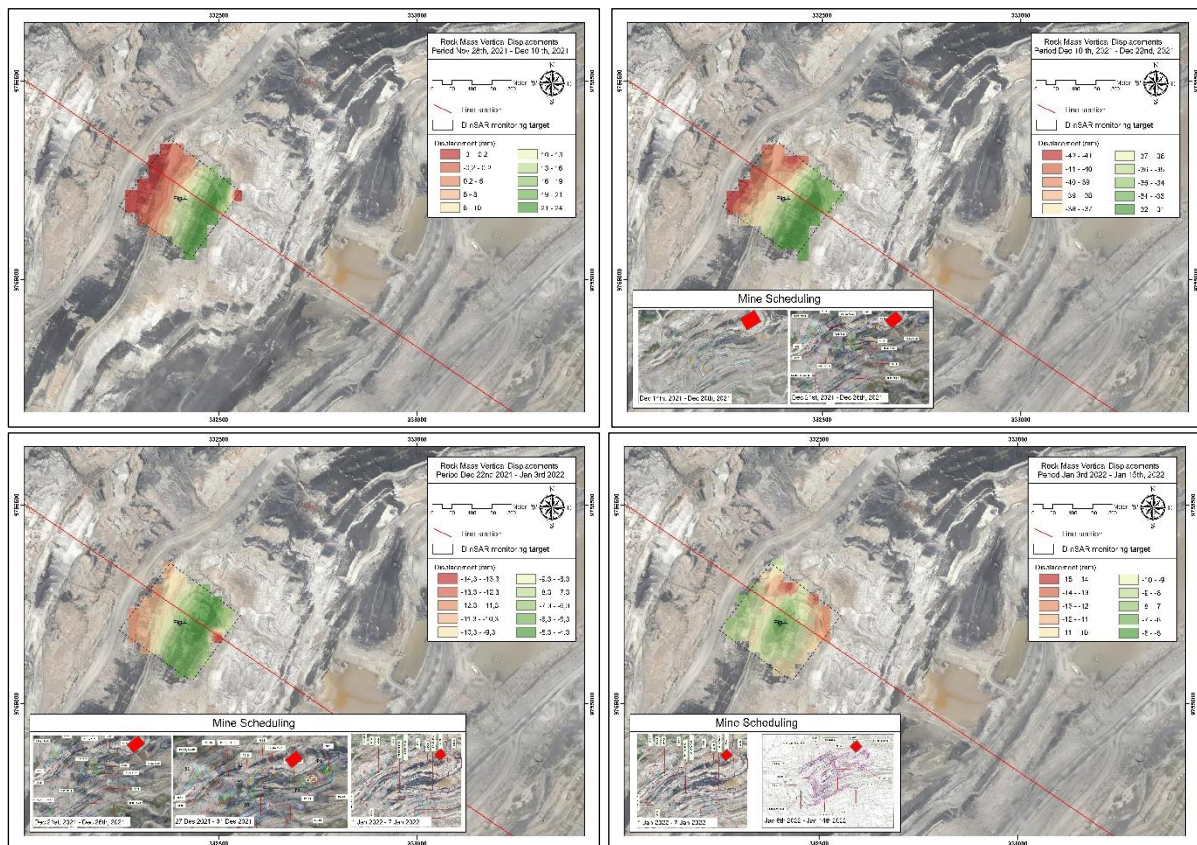


Figure 8 Regression graph of horizontal displacement based on ground-based radar monitoring and numerical analysis by Young's modulus reduction and applying the SRF method.

LoS Displacements Monitoring

To find the value of LoS displacement, the monitoring method used was D-InSAR analysis. Like the monitoring period to determine the value of horizontal displacement, the monitoring period to find the amount of LoS displacement was December 10th, 2021 to April 9th, 2022 with an interval of twelve days. Validation of the displacement values from the D-InSAR analysis was carried out on mining sequences. This was done because prism monitoring data was not available. Based on the mining sequence data during the monitoring period no mining was carried out in the area that was the monitoring target. Thus, the displacement detected by D-InSAR was not affected by the mining sequences.

The LoS displacement at the beginning of the period was known to be 3 mm. This value was obtained by comparing the topographic conditions in the Sentinel-1 data from December 10th, 2021 with the results from the previous data acquisition on November 28th, 2021. The same was done for each twelve-day time interval until the end of the monitoring period. On April 9th, 2022, the LoS displacement value was 50 mm. The results of the D-InSAR analysis for the monitoring period of December 10th, 2021 to April 9th, 2022 are presented in Figure 9. The LoS displacement value of the D-InSAR monitoring results is not an accumulation of displacement values. To compare them to the horizontal displacement values, the LoS displacement values were accumulated. All results of LoS displacement monitoring with D-InSAR are given in Table 4.



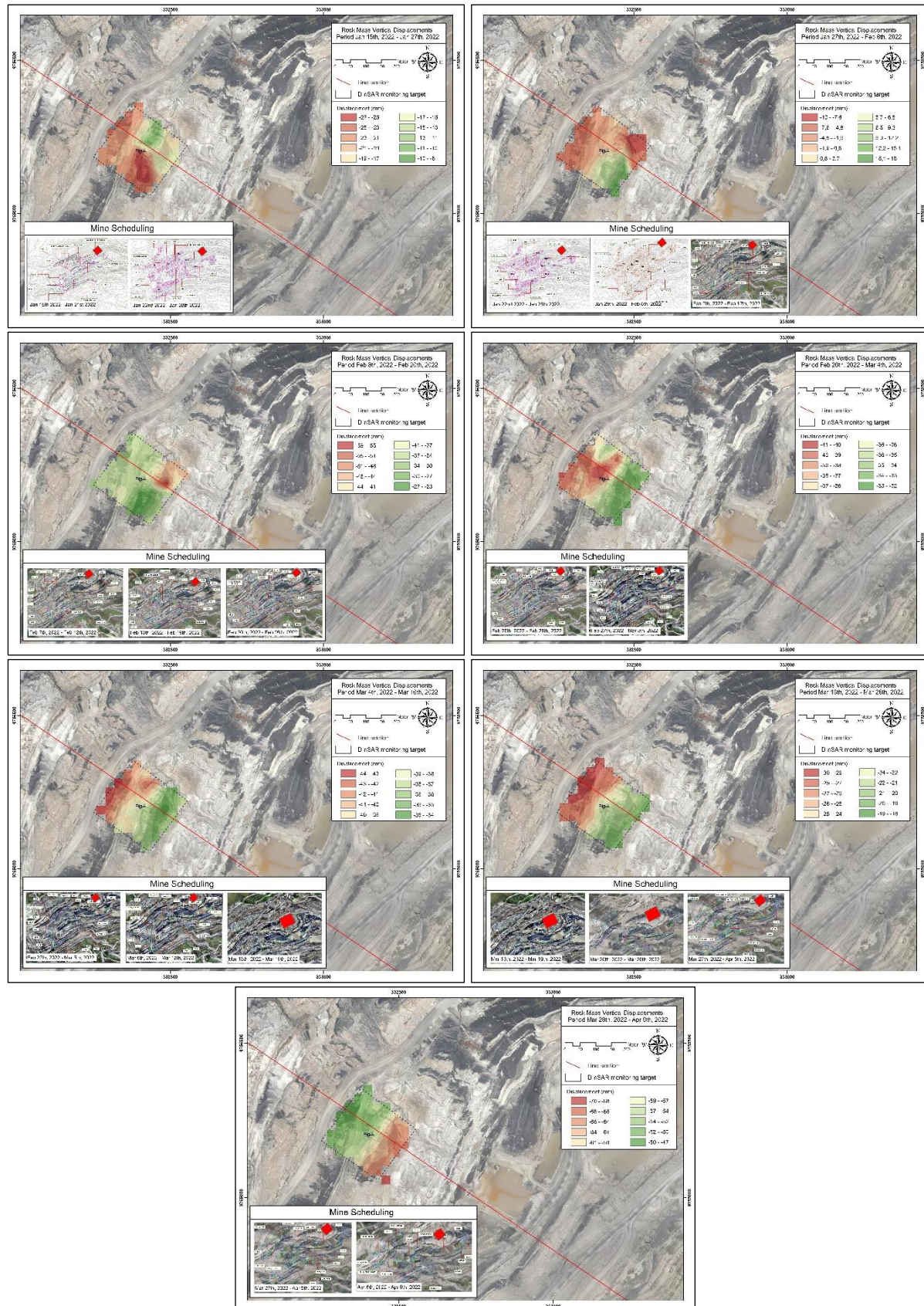


Figure 9 Continued. LoS displacement monitoring based on D-InSAR analysis from December 10th, 2021 to April 9th, 2022.

Table 4 LoS displacement values based on D-InSAR analysis from December 10th, 2021 to April 9th, 2022.

Date	LoS Displacements (mm)	
	D-InSAR	Cumulative
12/10/2021	-3.00	-3.00
12/22/2021	-42.00	-4500
01/03/2022	-11.30	-56.30
01/15/2022	-8.60	-64.90
01/27/2022	-23.00	-87.90
02/08/2022	-7.60	-95.50
02/20/2022	-34.00	-129.50
03/04/2022	-40.00	-169.50
03/16/2022	-43.00	-212.50
03/28/2022	-30.00	-242.50
04/09/2022	-50.00	-292.50

To determine the reduction of the Young's modulus values based on the LoS displacement values, numerical analysis was carried out. This numerical analysis was carried out with the same assumptions, namely variation of Young's modulus and the SRF method. Based on the results of the variation of Young's modulus, the LoS displacement value was found by reducing the Young's modulus value by 3% from the actual value of 18 mm. Variation of Young's modulus was continuously carried out until the LoS displacement values obtained from the numerical analysis were close to the results of D-InSAR monitoring. Based on these assumptions, the largest LoS displacement value obtained from the results of numerical analysis with a 35% reduction in the value of Young's modulus was 284 mm (Figure 10). The LoS displacement values resulting from the numerical analysis with the assumption of a complete reduction of Young's modulus are given in Table 5, while the results of the overall analysis in the form of a model are presented in Figure 10. Furthermore, a comparison graph of the LoS displacement values obtained from the numerical analysis and D-InSAR monitoring is presented in Figure 11.

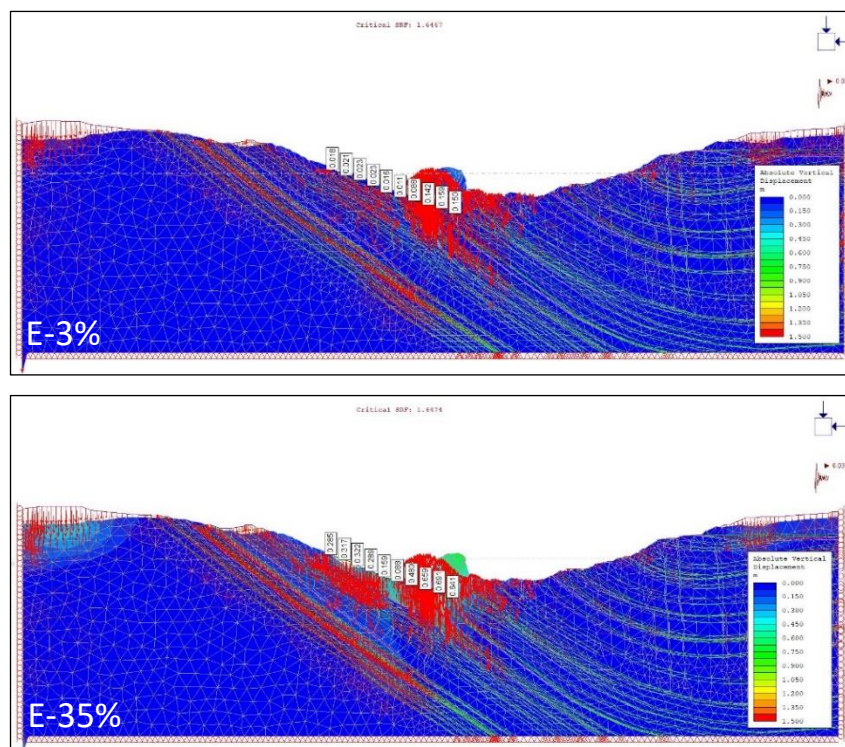
**Figure 10** LoS displacement based on numerical analysis by reduction of Young's modulus and applying the SRF method.

Table 5 Comparison of LoS displacement based on D-InSAR analysis and numerical analysis by reducing Young's modulus and applying the SRF method.

LoS Displacement Monitoring (mm)			LoS Displacement	SRF	Critical	Young's Modulus
Date	D-InSAR	Cumulative	Numerical Analysis (mm)	Displacement	SRF	Reduction (%)
12/10/2021	-3.00	-3.00	-18.00	1.300	1.647	E-3%
12/22/2021	-42.00	-45.00	-56.00	1.500	1.647	E-15%
01/03/2022	-11.30	-56.30	-58.00	1.500	1.648	E-18%
01/15/2022	-8.60	-64.90	-63.00	1.500	1.647	E-25%
01/27/2022	-23.00	-87.90	-107.00	1.600	1.648	E-27%
02/08/2022	-7.60	-95.50	-108.00	1.600	1.648	E-28%
02/20/2022	-34.00	-129.50	-141.00	1.625	1.648	E-29%
03/04/2022	-40.00	-169.50	-192.00	1.637	1.647	E-29.5%
03/16/2022	-43.00	-212.50	-197.00	1.637	1.648	E-30%
03/28/2022	-30.00	-242.50	-200.00	1.644	1.648	E-33%
04/09/2022	-50.00	-292.50	-284.00	1.644	1.648	E-35%

Based on the LoS displacement values obtained from the results of the D-InSAR analysis and the numerical analysis, a regression analysis was performed to determine the correlation between both analyses. The regression results are presented in Figure 11. The regression results show an R-square value of 0.9898. This value indicates that the LoS displacement value from the numerical analysis and from D-InSAR monitoring were correlated at 98.98%. In addition, other results came from a regression in the form of the following equation:

$$d_{vnum} = 1.0051d_{vDInSAR} \quad (2)$$

Where, d_{vnum} are the LoS displacement values resulting from the numerical analysis and $d_{vDInSAR}$ are the LoS displacement values based on the D-InSAR analysis.

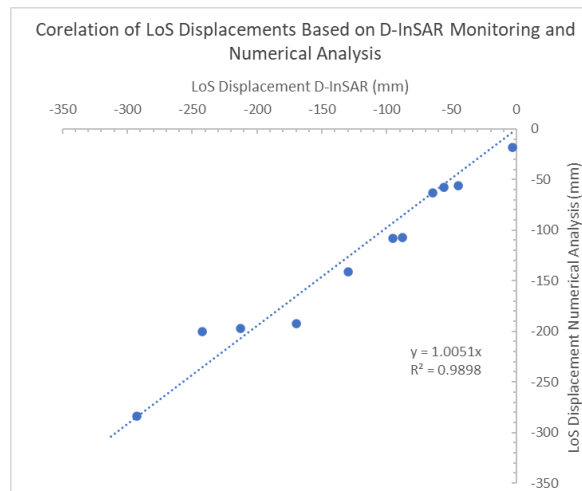


Figure 11 Regression graph of LoS displacement based on D-InSAR analysis and numerical analysis by reducing Young's modulus and applying the SRF method.

To determine the level of accuracy of the D-InSAR analysis, the trend formed from the displacement values of the D-InSAR monitoring results was compared to the trend of the ground-based radar monitoring results as shown in Figure 12. Overall, the two methods showed a constant or linear increase. The displacement trend based on the ground-based radar monitoring showed a significant increase at the beginning of the period. This may have been affected by noise in the ground-based radar data. Furthermore, correlation of the two methods showed an R-square value of 85% based on the following equation:

$$LoS_{disp} = 0.1419H_{disp} \quad (3)$$

Where the ground-based radar registered a horizontal displacement of around 1 mm, the D-InSAR analysis gave an LoS displacement of around 0.1419 mm with an R-square of 85%.

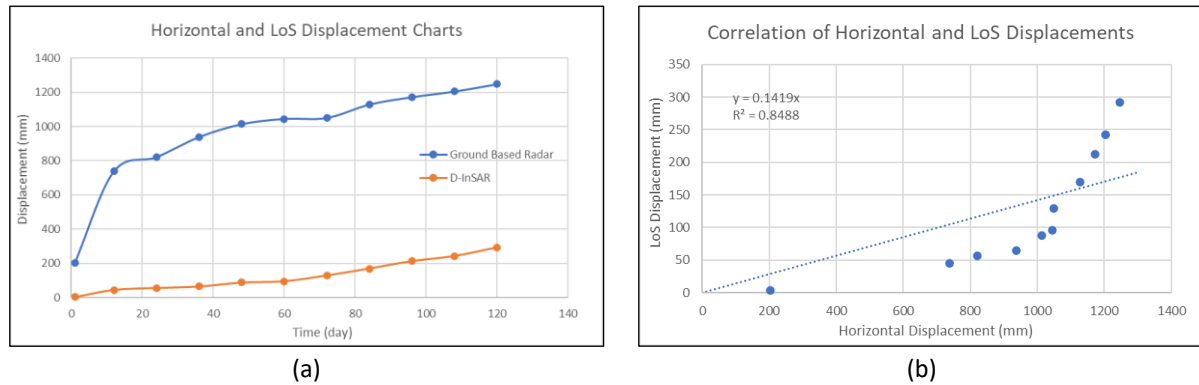


Figure 12 (a) Horizontal and LoS displacement charts; (b) correlation of horizontal and LoS displacements.

Discussion

Based on the results of horizontal and LoS displacement monitoring, it was found that the displacement values increased. In line with these conditions, the results of the numerical analysis also showed an increase in the displacement values, one of which was caused by a decrease in the Young's modulus value of the material. In the numerical analysis that was carried out, to obtain a displacement value that is close to the monitoring results, the Young's modulus value for each material was reduced by 3% to 35%. As one of the parameters of rock mechanics, changes in Young's modulus are influenced by the heating-cooling cycles of the rock. This can cause rock to experience deterioration so that it experiences a decrease in strength [8]. The intensity of light and high rainfall in areas located around the equator make this cycle faster.

In this study, the reduction in the Young's modulus value was calculated based on a monitoring period for horizontal and LoS displacement from December 10th, 2021 to April 9th, 2022, as fully described in Table 6. At the beginning of the monitoring period, the Young's modulus value had decreased by 3%, as is known from the results of the numerical analysis. This value continued to increase until the end of the monitoring period, where the percentage of Young's modulus reduction was 35%. Based on these assumptions, this study also conducted a regression to determine the decrease in the Young's modulus value as a function of time. The results of the regression are presented in Figure 13, which shows an R-square value of 0.9609. In addition, an equation was obtained to determine the percentage of reduction in Young's modulus of the material in the South Tutupan pit at the following monitoring time intervals:

$$E_{red}(\%) = -6.575 \ln(day) - 0.8916 \quad (4)$$

where, $E_{red}(\%)$ is the percentage of Young's modulus reduction, and day is the day of monitoring as the time.

Table 6 Percentage of Young's modulus reduction based on horizontal displacement and LoS displacement monitoring from December 10th, 2021 to April 9th, 2022.

Date	Day	Horizontal Displacement (mm)				LoS Displacement (mm)			Yung's Modulus Reduction
		GBR	Numerical Analysis			D-InSAR Analysis		Numerical Analysis	
			Low wall	High wall	Sum	D-InSAR	Cumulative		
10/12/2021	1	202.28	205.00	76.00	281.00	-3.00	-3.00	-18.00	E-3%
22/12/2021	12	737.59	644.00	119.00	763.00	-42.00	-45.00	-56.00	E-15%
03/01/2022	24	821.33	741.00	122.00	863.00	-11.30	-56.30	-58.00	E-18%
15/01/2022	36	938.53	791.00	135.00	926.00	-8.60	-64.90	-63.00	E-25%
27/01/2022	48	1013.79	888.00	139.00	1027.00	-23.00	-87.90	-107.00	E-27%
08/02/2022	60	1044.68	894.00	140.00	1034.00	-7.60	-95.50	-108.00	E-28%
20/02/2022	72	1050.47	904.00	142.00	1046.00	-34.00	-129.50	-141.00	E-29%
04/03/2022	84	1128.49	984.00	144.00	1128.00	-40.00	-169.50	-192.00	E-29.5%
16/03/2022	96	1171.74	1027.00	145.00	1172.00	-43.00	-212.50	-197.00	E-30%
28/03/2022	108	1204.60	1033.00	151.00	1184.00	-30.00	-242.50	-200.00	E-33%
09/04/2022	120	1247.34	1098.00	156.00	1254.00	-50.00	-292.50	-284.00	E-35%

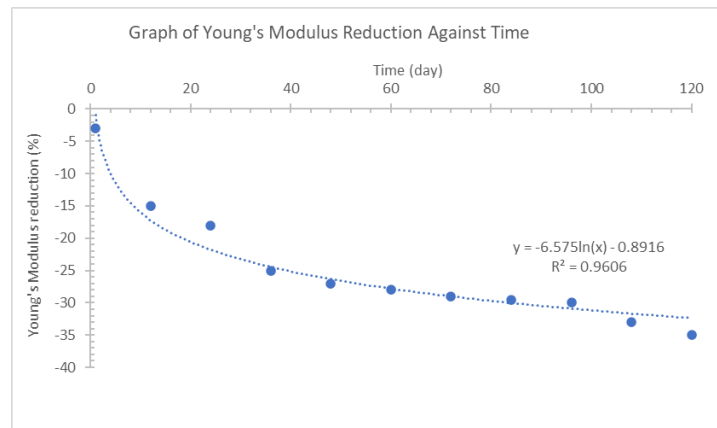


Figure 13 Regression graph of Young's modulus reduction against time.

Based on the Young's modulus reduction values in Table 6 and the regression results in Figure 13, it is known that the Young's modulus values decreased significantly at the beginning of the monitoring period. In line with increasing time, the decreasing trend in Young's modulus was not significant until the end of the monitoring period with a decrease percentage value of 5%. There was a decrease in the Young's modulus value in the South Tutupan Pit low wall area, caused among others by heating-cooling cycles. This phenomenon causes several components in rocks to change. One component that changes due to the heating-cooling cycle is the mineral composition of the rocks. A type of mineral that can be found in large quantities in almost all types of rocks is quartz. Rocks with a predominantly quartz composition can experience a rapid change in Young's modulus at a temperature interval of 25°C to 520°C [8]. This shows when temperatures are not too high, changes in Young's modulus can occur. When correlated with the conditions in the study area, the increase in temperature due to heat from sunlight could be one of the factors causing a decrease in the value of Young's modulus in the rocks.

In addition to changes the mineral contents, the heating-cooling cycle can also affect the presence of microcracks in rocks. In sedimentary rocks, microcracks appear in the gaps between the grains that make up the rock. If the rock undergoes a rapid heating-cooling cycle, it will cause the constituent grains to shrink. This shrinkage will be the initiator of the formation of microcracks. In line with the formation of more and more microcracks, the Young's modulus value of the rock will also decrease.

Conclusion

To determine the displacement value, two methods were used, namely ground-based radar monitoring for horizontal displacement and D-InSAR analysis for LoS displacement. Meanwhile, to determine the Young's modulus value of the rock mass, finite element numerical analysis was carried out by reducing the value of Young's modulus to obtain displacement value that are close to those from the monitoring results. In line with the increase in the horizontal and LoS displacement values that were known based on monitoring, the results of the numerical analysis also showed a reduction of the Young's modulus value for each material. Based on the results of the analysis, it was found that the Young's modulus value was reduced by 3% on December 10th, 2021 and continued decrease to 35% on April 9th, 2022. Based on the results of the analysis, it is known that the decrease in the value of Young's modulus is related to heating-cooling cycles in the research area.

References

- [1] Botin, J.A., *Sustainable Management of Mining Operations*, Society for Mining, Metallurgy, and Exploration, Inc. Colorado, 2009.
- [2] Dick, G.J., Eberhardt, E., Cabrejo-Lievano, A.G., Stead, D. & Rose, N.D., *Development of an Early-Warning Time of Failure Analysis Methodology for Open Pit Mine Slopes Utilizing Ground Based Slope Stability Radar Monitoring Data*, Canadian Geotechnical Journal, **52**(4), pp.1-15, 2014.
- [3] Paradella, W.R., Ferretti, A., Mura, J.C., Colombo, D., Gama, F.F., Tamburini, A., Santos, A.R., Novali, F., Galo, M., Camargo, P.O., Silva, A.Q., Silva, G.G., Silva, A. & Gomes, L.L., *Mapping Surface Deformation in Open Pit Iron*

mines of Carajás Province (Amazon Region) Using an Integrated SAR Analysis. Engineering Geology.193, pp. 61-78, 2015.

[4] Broadbent, C.D. & Zavodni, Z.M., *Influence of Rock Structure on Stability*, in *Stability in Surface Mining*, **3**(2), Society of Mining Engineers, Denver, CO, 1982.

[5] Pepe, A. & Calò, F., *A Review of Interferometric Synthetic Aperture RADAR (InSAR) Multi-track Approaches for The Retrieval of Earth's Surface Displacements*, in Applied Sciences (Switzerland), **7**(12), 1264, 2017. doi: 10.3390/app7121264.

[6] Vyalov, S.S., *Rheological Fundamental of Soil Mechanics*, Elsevier, 1986.

[7] Serco Italia SPA, *Volcano Monitoring with Sentinel-1*. (Version 1.1). Retrieved from RUS Lectures at <https://rus-copernicus.eu/portal/the-rus-library/train-with-rus/>, (April 20, 2022).

[8] Liu, W., Zhang, L. & Luo, N., *Elastic Modulus Evolution of Rocks Under Heating-Cooling Cycles*, Nature Scientific Reports, **10**(1), 13835, 2020. doi: 10.1038/s41598-020-70920-3.

Manuscript Received: 1 October 2022

1st Revision Manuscript Received: 21 November 2022

2nd Revision Manuscript Received: 20 December 2022

3rd Revision Manuscript Received: 18 March 2023

Accepted Manuscript: 3 May 2023